Euro. Jnl of Applied Mathematics (2000), *vol.* 11, *pp.* 171–179. Printed in the United Kingdom

© 2000 Cambridge University Press

The distortion of a bubble in a corner flow

E. OZUGURLU[1] and J.-M. VANDEN-BROECK[2]

[1]*Department of Mathematics and Center for the Mathematical Sciences, University of Wisconsin-Madison, WI 53706, USA*
[2]*School of Mathematics, University of East Anglia, Norwich NR4 7TJ, UK*

(*Received 23 November 1998; revised 18 June 1999*)

The distortion of a two-dimensional bubble (or drop) in a corner flow of an inviscid incompressible fluid is considered. Numerical solutions are obtained by series truncation. The results confirm and extend previous calculations.

1 Introduction

Over the years many solutions have been obtained for the deformation of two dimensional bubbles in a flow. Both steady and unsteady solutions were considered. Here we concentrate our attention to steady solutions, (see, for example, Baker & Moore [1], and the references cited in that paper for time dependent solutions).

McLeod [4] obtained an exact solution for a free bubble rising in a fluid. Vanden-Broeck & Keller [12] showed numerically that McLeod's solution is a member of a one parameter family of solutions. They also solved the flow past a bubble attached to a wall (i.e. the configuration of Figure 1 with $\alpha = \pi$). This problem was also considered by Meiron [5], Shankar [6] and Tanveer [7]. Vanden-Broeck & Keller [13] considered the related problem of the deformation of a bubble attached to the walls of a rectangular wedge (i.e. the configuration of Figure 1 with $\alpha = \pi/2$). When reflected into the walls, this configuration models the distortion of a bubble in a straining flow.

The solutions in Vanden-Broeck & Keller [12, 13] were obtained numerically by boundary integral equation methods. It was found that the families of solutions ultimately approach limiting configurations in which opposite sides of the bubble touch each other. In Vanden-Broeck & Keller [13], numerical solutions were not obtained close to the limiting configuration, and an approximate analytical solution was derived to describe the limiting configuration. This approximate solution was extended to other values of α in Vanden-Broeck [8]. It was also shown [8] that solutions can be found past the limiting configurations by forcing contact of the opposite sides at one point or along a segment.

In this paper, we present another numerical procedure to compute solutions for the flow configuration of Figure 1. The scheme is based on series truncation, and is similar in philosophy (if not in details) to those used by Vanden-Broeck [9–11] and Daboussy *et al.* [3]. Numerical solutions are obtained for all values of α and of the contact angle β. The results of Vanden-Broeck & Keller [12, 13] are recovered for $\alpha = \pi$ and $\alpha = \pi/2$. In

https://doi.org/10.1017/S0956792599003940 Published online by Cambridge University Press

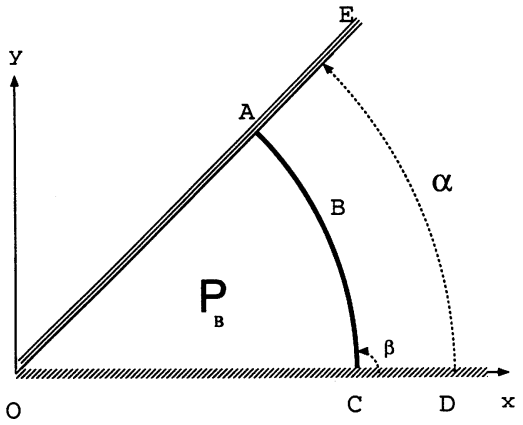


FIGURE 1. Sketch of the flow and coordinates.

addition, the results of Vanden-Broeck & Keller [13] are extended numerically up to the limiting configuration.

The solutions for values of α not equal to π or $\pi/2$ are not covered in the calculations of Vanden-Broeck & Keller [12, 13], although approximate solutions based on slender body theory were derived [8]. The fully nonlinear solutions derived in this paper are of interest, since flows in wedges have recently been used to model the flow in a crack in a seawall struck by a wave [2]. The present calculations provide an additional model for cracks by allowing a trapped bubble at the apex of the wedge.

The problem is formulated in § 2. The numerical procedure is described in § 3 and the numerical results are presented in § 4.

2 Formulation of the problem

We consider the two-dimensional flow configuration shown in Figure 1. The flow domain is bounded by the two walls AE and CD and by the free surface AC. The fluid is assumed to be inviscid and incompressible, and the flow to be irrotational and steady. We take into account the effect of the surface tension T at the interface, but we ignore the flow inside the bubble $OACO$, assuming that the pressure is a constant P_B throughout it. The angle between the two walls is denoted by α, and the contact angle between walls and the free surface is denoted by β (see Figure 1). We introduce Cartesian coordinates with the origin at the intersection of the two walls and the x-axis along the wall CD.

We introduce the potential function ϕ and the streamfunction ψ. We choose $\psi = 0$ along the walls and along the bubble and $\phi = 0$ at the point B in the middle of the free surface profile (see Figure 1). We denote by $\pm b$ the values of ϕ at C and A. Next, we define dimensionless variables by taking $T/(\rho b)$ as the reference velocity and $\rho b^2/T$ as the unit length. Then the flow region corresponds to the upper half (i.e. $\psi \geqslant 0$) of the (ϕ, ψ) plane. The bubble surface corresponds to the segment $-1 < \phi < 1, \quad \psi = 0$ of the ϕ axis (see Figure 2).

https://doi.org/10.1017/S0956792599003940 Published online by Cambridge University Press

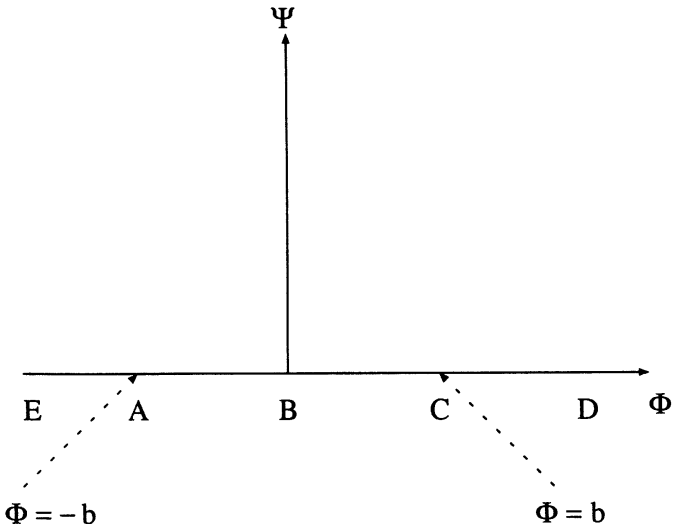


FIGURE 2. The complex potential plane.

On the free surface AC, Bernoulli's equation yields

$$\tfrac{1}{2}(u^2+v^2)-\frac{T}{\rho}K=\frac{p_S-p_B}{\rho}, \tag{1}$$

where u and v denote the x and y components of the velocity, K is the curvature of the free surface, and p_S is the stagnation pressure.

In terms of our dimensionless variables, we rewrite (1) as

$$\tfrac{1}{2}(u^2+v^2)-K=\xi, \tag{2}$$

where

$$\xi=\frac{\rho b^2}{T^2}\quad(p_S-p_B). \tag{3}$$

The kinematic boundary conditions on the walls yield

$$v=0\quad\text{on}\quad CD, \tag{4a}$$

and

$$v=u\tan\alpha\quad\text{on}\quad AE. \tag{4b}$$

Finally, we impose a contact angle β at $\phi=\pm1$ by the relations

$$v=u\tan\beta\quad\text{at}\quad\phi=1, \tag{5a}$$

$$v=-u\tan(\beta-\alpha)\quad\text{at}\quad\phi=-1. \tag{5b}$$

In (5a) and (5b), the angle β is assumed to be prescribed.

This completes the formulation of the problem. We seek $u-iv$ as an analytic function of $f=\phi+i\psi$ in the lower half plane $\psi<0$ satisfying equations (2), (4) and (5).

https://doi.org/10.1017/S0956792599003940 Published online by Cambridge University Press

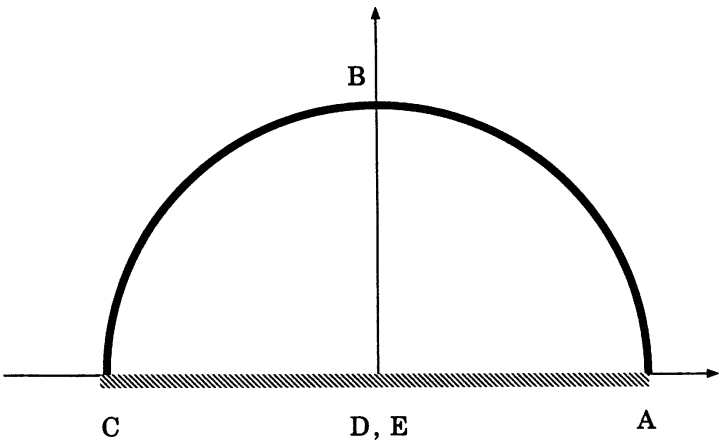


FIGURE 3. The complex t-plane.

3 Numerical procedure

In this section we derive a numerical scheme based on series truncation to solve the problem of Figure 1. The scheme supplements the work of Vanden-Broeck & Keller [12, 13], where solutions for $\alpha = \pi$ and $\alpha = \pi/2$ were calculated by boundary integral equation methods.

We first map the flow domain into the inside of a unit disk in the complex t-plane by the transformation

$$f = -\frac{1+t^2}{2t}. \tag{6}$$

This transformation maps the walls on the real diameter and the free surface on the unit circle (see Figure 3). The point B in Figures 2 and 3 is the point on the free surface where $\phi = 0$. We shall seek solutions which are symmetric with respect to B.

We denote the complex velocity by $\zeta = u - iv$. We consider ζ as a function of t. Since there are angled corners at $t = \pm 1$, ζ has singularities at these points. The appropriate singularities are

$$\zeta \sim (t \mp 1)^{2-\frac{2\beta}{\pi}} \quad \text{as} \quad t \to \pm 1. \tag{7}$$

Furthermore as $t \longrightarrow 0$,

$$f \sim \left(\frac{1}{t}\right)^{1-\frac{\alpha}{\pi}}. \tag{8}$$

We represent the complex potential ζ by the expansion

$$\zeta = (1-t^2)^{2-\frac{2\beta}{\pi}} \left(-\frac{1}{t}\right)^{1-\frac{\alpha}{\pi}} \sum_{n=1}^{\infty} a_n t^{n-1}. \tag{9}$$

The kinematic conditions (4) on the walls AE and CD imply that the coefficients a_n are real. It can be checked that (9) satisfies (4) and (5). Therefore, we can expect the series in (9) to converge for $|t| < 1$. The coefficients a_n must be determined to satisfy the condition (2) on the free surface AC.

We use the notation $t = \mid t \mid e^{i\sigma}$ so that points on AC are given by $t = e^{i\sigma}$, where

https://doi.org/10.1017/S0956792599003940 Published online by Cambridge University Press

$0 \leqslant \sigma \leqslant \pi$. Using (6), we find that $\phi = -\cos(\sigma)$ on the free surface. Since

$$\frac{\partial x}{\partial \phi} + i\frac{\partial y}{\partial \phi} = \frac{1}{u - iv} = \frac{u + iv}{u^2 + v^2}, \tag{10}$$

we can then write the curvature as

$$K = -\frac{1}{\sin(\sigma)} \frac{uv_\sigma - vu_\sigma}{\sqrt{u^2 + v^2}}, \tag{11}$$

and Bernoulli's equation (2) yields

$$\tfrac{1}{2}(u^2 + v^2) + \frac{1}{\sin(\sigma)} \frac{uv_\sigma - vu_\sigma}{\sqrt{u^2 + v^2}} = \xi \tag{12}$$

on the free surface AC.

We solve the problem approximately by truncating the infinite series in (9) after $N - 2$ terms. Thus, we write

$$\zeta \sim (1 - t^2)^{2 - \frac{2\beta}{\pi}} \left(-\frac{1}{t}\right)^{1 - \frac{\alpha}{\pi}} \sum_{n=1}^{N-2} a_n t^{n-1}, \tag{13}$$

and we introduce the $N - 2$ collocation points

$$\sigma_I = \pi \frac{I - 1/2}{N - 2}, \quad I = 1, ..., N - 2. \tag{14}$$

Substituting $t = e^{i\sigma_I}$ into (13) and taking the real and imaginary parts, we obtain the values of u and v at the mesh points (14) in terms of the coefficients a_n. Similarly, we substitute $t = e^{i\sigma}$ into (13), differentiate with respect to σ, and take the real and imaginary parts to obtain u_σ and v_σ at the mesh points (14) in terms of a_n. Substituting these values in (12) evaluated at the mesh points (14), we have $N-2$ equations for the $N-1$ unknowns ξ and a_n, $n = 1, \ldots, N - 2$. We obtain one more equation by fixing an extra parameter δ. Here we choose

$$\delta = -\xi \frac{2^{\alpha/(2\pi - \alpha)}}{a_1^{2\pi/(2\pi - \alpha)}}. \tag{15}$$

The last equation is then given by (15), where the left-hand side is given. The particular choice (15) is motivated by the fact that (15) reduces to the parameters γ used in Vanden-Broeck & Keller [12, 13] when $\alpha = \pi$ and $\alpha = \pi/2$. This facilitates comparisons. For given values of α, β and δ, the system of $N - 1$ nonlinear algebraic equations with $N - 1$ unknowns is solved by Newton's method. Once a solution was obtained for given values of α, β and δ, a continuation method was used (i.e. the solution was used as an initial guess to compute a new solution for perturbed values of the parameters α, β and δ and so on).

4 Discussion of results

We used the numerical scheme described in § 3 to compute solutions for given values of α, β and δ. The coefficients a_n were found to decrease very rapidly. For example, for $\alpha = \beta = \pi/2$ and $\delta = -1.3$, $a_1 \approx 0.93$, $a_{11} \approx -0.36$, $a_{21} \approx 0.028$, $a_{41} \approx 0.000095$ and $a_{65} \approx 0.000000072$. Most of the results presented in this paper were obtained with $N = 160$.

https://doi.org/10.1017/S0956792599003940 Published online by Cambridge University Press

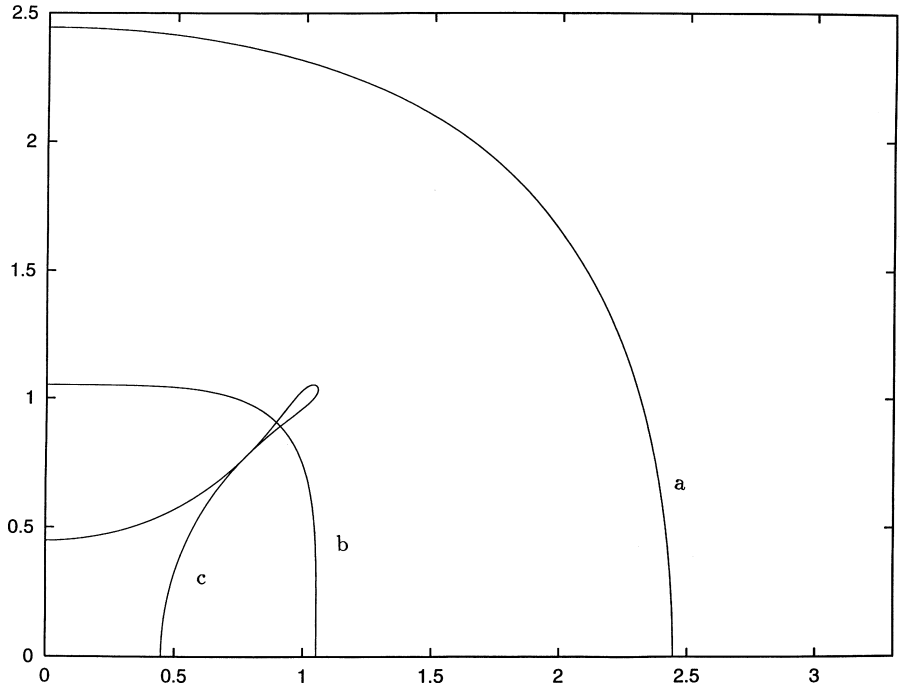


FIGURE 4. Free surface profiles for (a) $\alpha = \pi/2$ and $\beta = \pi/2$ with $\delta = 1$, (b) $\delta = 0$ and (c) $\delta = \delta_0 = -1.3$.

Typical free surface profiles are shown in Figures 4–6. As $\delta \to \infty$, the bubble tends to a circular arc. It is easily shown that it is consistent with (2) and (15). As $\delta \to \infty$, $\xi \to -\infty$ and (2) implies that $K \to -\xi$. Therefore, the bubble profile approaches an arc of a circle of radius $-1/\xi$ as $\delta \to \infty$. As δ decreases the bubble elongates in the direction which bisects the angle α. When δ reaches a certain value $\delta_0(\beta, \alpha)$, opposite sides of the bubble touch each other. For $\beta \leqslant \alpha/2$ this point of contact is at the intersection of the two walls (see Figure 6), while for $\beta > \alpha/2$ it is off the walls (see Figures 4 and 5).

The solutions for $\alpha = \pi$ were previously calculated elsewhere [3–6]. For $\beta \neq \pi/2$, they model the deformation of a bubble attached to a wall. For $\beta = \pi/2$ they also represent half of free bubble.

In Vanden-Broeck & Keller [13], solutions for $\alpha = \pi/2$ and $\delta > -1.24$ were obtained by a boundary integral equation method. Here these results are extended up to the value $\delta = -1.3$ at which opposite sides of the bubble touch at one point (see Figure 4).

Finally, let us mention that our scheme can also be used to compute solutions for $\alpha > \pi$. It corresponds to a flow around a corner with a bubble attached at its apex. A typical profile is shown in Figure 7. We note that the velocity is finite everywhere along the streamline $\psi = 0$. This is to be contrasted with the flow in the absence of a bubble, for which the velocity is infinite at the apex of the corner.

https://doi.org/10.1017/S0956792599003940 Published online by Cambridge University Press

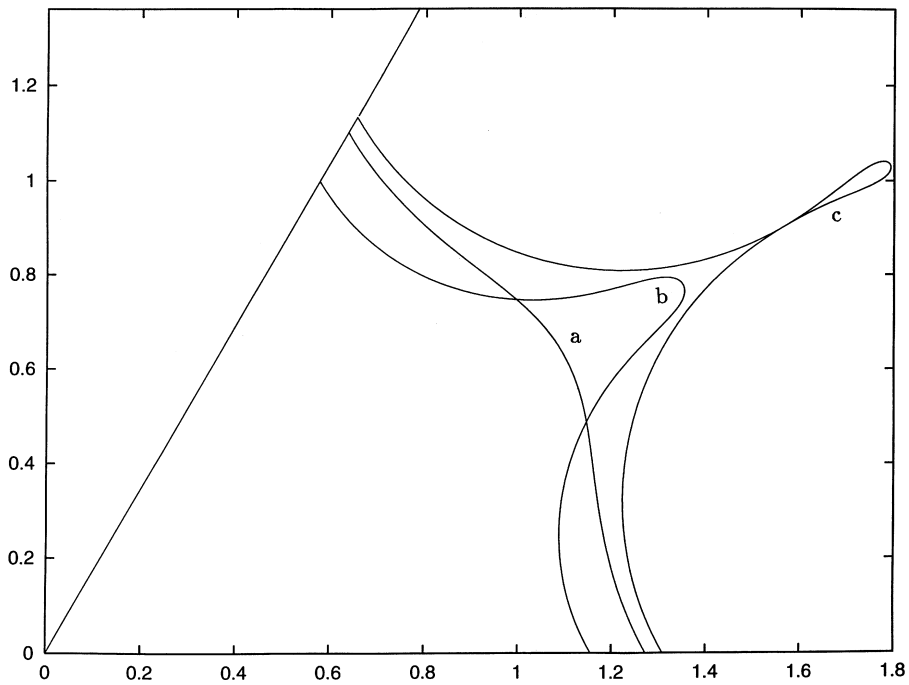


FIGURE 5. Free surface profiles for (a) $\alpha = \pi/3$ and $\beta = 2\pi/3$ with $\delta = -1.35$, (b) $\delta = -2.0$ and (c) $\delta = \delta_0 = -2.05$.

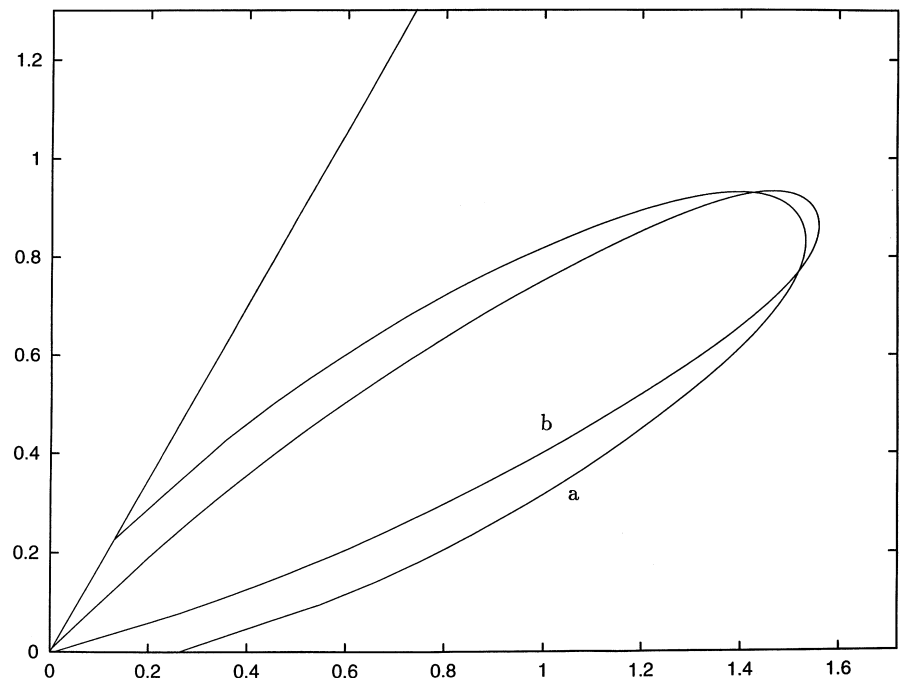


FIGURE 6. Free surface profiles for (a) $\alpha = \pi/3$ and $\beta = \pi/12$ with $\delta = 0.5$ and (b) $\delta = \delta_0 = 0.32$.

https://doi.org/10.1017/S0956792599003940 Published online by Cambridge University Press

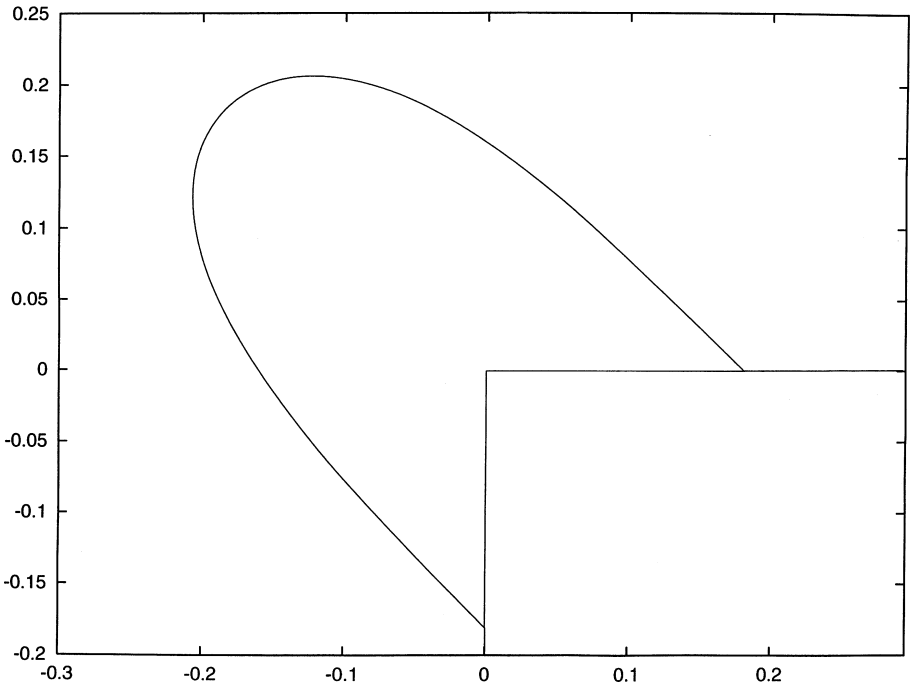


FIGURE 7. Free surface profile for $\alpha = 3\pi/2$, $\beta = 3\pi/4$ and $\delta = 0$.

5 Conclusions

We have used a series truncation method to calculate the deformation of a bubble in a corner flow. Our results include as particular cases those Vanden-Broeck & Keller [12, 13]. We were able to extend the calculations up to the limiting configurations, where opposite sides of the bubbles touch each other.

References

[1] BAKER, G. R & MOORE, D. W. (1989) The rise and distortion of a two-dimensional bubble in an inviscid liquid. *Phys. Fluids* **A1**, 1451–1459.

[2] COOKER, M. (1999) Potential flow for a steady jet in a wedge. *Quart. J. Mech. Appl. Math.* (in press).

[3] DABOUSSY, D., DIAS, F. & VANDEN-BROECK, J.-M. (1998) Gravity flows with a free surface of finite extent. *Euro. J. Mech. B/Fluids*, **17**, 19–31.

[4] MCLEOD, E. B. (1955) The explicit solution of a free boundary problem involving surface tension. *J. Rat. Mech. Analysis* **4**, 557–567.

[5] MEIRON, D. I. (1989) On the stability of gas bubbles rising in an inviscid fluid. *J. Fluid Mech.* **198**, 101–114.

[6] SHANKAR, P. N. (1992) On the shape of a two-dimensional bubble in uniform motion. *J. Fluid Mech.* **244**, 187–200.

[7] TANVEER, S. (1996) Some analytical properties of solutions to a two-dimensional steadily translating inviscid bubble. *Proc. R. Soc. Lond. A*, **452**, 1397–1410.

[8] VANDEN-BROECK, J.-M. (1981) Bubble in a corner flow. *Proc. 2nd Int. Coll. on Drops and Bubbles*, Monterey, CA, pp. 336–343.

https://doi.org/10.1017/S0956792599003940 Published online by Cambridge University Press

[9] Vanden-Broeck, J.-M. (1984) The effect of surface tension on the shape of the Kirchoff jet. *Phys. Fluids*, **27**, 1933–1936.
[10] Vanden-Broeck, J.-M. (1984) Rising bubbles in a two-dimensional tube with surface tension. *Phys. Fluids*, **27**, 2604–2607.
[11] Vanden-Broeck, J.-M. (1989) Bow flows in water of finite depth. *Phys. Fluids*, **A1**, 1328–1330.
[12] Vanden-Broeck, J.-M. & Keller, J. B. (1980) Deformation of a bubble or drop in a uniform flow. *J. Fluid Mech.* **101**, 673–686.
[13] Vanden-Broeck, J.-M. & Keller, J. B. (1980) Bubble or drop distortion in a straining flow in two dimensions. *Phys. Fluids*, **23**, 1491–1495.

https://doi.org/10.1017/S0956792599003940 Published online by Cambridge University Press